

**OPEN ACCESS**

## Neutron beam focusing using large-m supermirrors coated on precisely-figured aspheric surfaces

To cite this article: D Yamazaki *et al* 2010 *J. Phys.: Conf. Ser.* **251** 012076

View the [article online](#) for updates and enhancements.

### You may also like

- [New polarizing guide for neutron wavelengths above 2.5 Å](#)  
Th Krist, C Pappas, A Teichert et al.
- [Design and Fabrication of Ni/Ti Multilayer for Neutron Supermirror](#)  
Zhang Zhong, Wang Zhan-Shan, Zhu Jing-Tao et al.
- [Self-shielding copper substrate neutron supermirror guides](#)  
P M Bentley, R Hall-Wilton, C P Cooper-Jensen et al.



**ECS**  
The  
Electrochemical  
Society  
Advancing solid state &  
electrochemical science & technology

**DISCOVER**  
how sustainability  
intersects with  
electrochemistry & solid  
state science research

# Neutron beam focusing using large- $m$ supermirrors coated on precisely-figured aspheric surfaces

D. Yamazaki<sup>1</sup>, R. Maruyama<sup>1</sup>, K. Soyama<sup>1</sup>, H. Takai<sup>2</sup>, M. Nagano<sup>2</sup>  
and K. Yamamura<sup>2</sup>

<sup>1</sup> J-PARC Center, Japan Atomic Energy Agency, Tokai-mura, Ibaraki 319-1195, Japan

<sup>2</sup> Research Center for Ultra-precision Science and Technology, Osaka University, Osaka 565-0871, Japan

E-mail: yamazaki.dai@jaea.go.jp

**Abstract.** We have developed a 1-dimensional elliptic mirror combining a supermirror coated with ion-beam sputtering and precise elliptic surface figured with the numerically-controlled local wet etching process. In this study, NiC/Ti supermirror ( $m=4$ ) was deposited on a precisely figured surface of synthesized quartz glass over  $90\text{ mm} \times 40\text{ mm}$ . Wideband neutrons of  $\lambda > 3.64\text{ \AA}$  were focused with focal spot size down to  $0.25\text{ mm}$ , peak intensity gain up to 6 without significant diffuse scattering. Time-of-flight measurements suggest that wideband neutrons are effectively focused to the focal point.

## 1. Introduction

In recent years, there have been major developments of new neutron facilities including J-PARC, SNS and ISIS TS2. The new or upgraded sources will provide higher neutron intensity than ever. Nevertheless the intensities are still low compared to that of X-ray facilities. Neutron beam focusing devices are, therefore, indispensable in these facilities to accommodate micrometer-scale samples and second-resolution time-resolved measurements. As for focusing devices at spallation neutron sources, achromatic optics are particularly important because most experiments are performed with wideband beams. Reflective focusing is a prominent candidate for that purpose.

A focusing mirror needs to accept and reflect wideband beam with large divergence into small area with high efficiency and high signal-to-noise ratio. In order to meet these demands required are (1) large critical angle of total reflection, (2) high reflectivity, (3) low diffuse scattering, (4) large dimension and (5) precise surface figure of the focusing mirror. The low diffuse scattering (3) is particularly important to focus the beam on to a detector surface in order for small-angle scattering (SANS) or grazing-incidence SANS.

Ice and coworkers have developed focusing devices by bending a flat supermirror into approximately elliptic shape [1, 2]. Their devices utilize  $m = 3$  supermirror deposited on flat substrates and have realized 2-dimensional focusing onto a  $90\text{ }\mu\text{m}$  spot. ( $m$  denotes the ratio of the total-reflection critical angle of the supermirror to that of natural nickel.)

We have been developing ultra-precise focusing mirrors combining high-performance neutron supermirror and very precise surface figuring technique. We have already developed high-performance neutron supermirrors using ion-beam sputtering (IBS) process. Reflectivities 0.88 at  $m = 3$ , 0.82 at  $m = 4$  and 0.40 at  $m = 6$  have been achieved [3] with low diffuse scattering

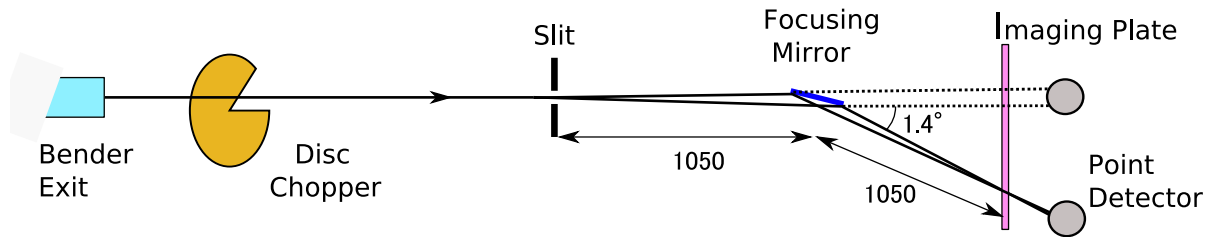


**Figure 1.** Experimental setup.

[4]. Critical angle up to  $m = 6.7$  has also been demonstrated [5]. Mirrors can be deposited over a range of 500 mm in diameter. On the other hand, high-precision surfaces figurings have been realized over a large area using the numerically controlled local wet etching (NC-LWE) process [6, 7]. Peak-to-valley flatness down to 69 nm has been achieved over  $142 \times 142$  mm. In this letter, a fabrication of a 1-dimensional elliptic neutron supermirror and a performance test using wideband neutron beam are reported.

## 2. Mirror Fabrication

A mirror substrate was prepared by figuring a surface of synthesized quartz glass into a plano-elliptical shape using the NC-LWE process. The ellipsoid is of  $x^2/(1050.31)^2 + z^2/(25.66)^2 = 1$ , where the units of  $x$  and  $z$  are mm. The focal length is 1050 mm. The aperture size is 90 mm (elliptic)  $\times$  40 mm (straight) and it covers eccentric angle  $87.55 < \theta < 92.45$  deg of the ellipsoid. NiC/Ti supermirror ( $m = 4$ ) was deposited using the IBS method on the elliptic quartz surface.

The elliptic mirror is supposed to accept a neutron beam with nominal glancing angle of 1.40 deg and reflect and focus wideband neutrons with wavelength  $\lambda \geq 3.5 \text{ \AA}$ . The acceptance angle, therefore, is 0.12 deg. Details of the fabrication are described elsewhere [8, 9] together with a test result of monochromatic beam focusing .

## 3. Experimental Results and Discussions

Wideband neutron beam focusing was demonstrated on the CHOP beam port of JRR-3. CHOP provides a neutron beam of  $\lambda \geq 3 \text{ \AA}$  which is bent by 20 degrees with a multi-channel cold neutron bender [10] at the end of the C-2 guide tube.

The beam-line is illustrated in Fig. 1. The focusing mirror was placed at an angle of  $\sim 1.4$  deg to the beam line. A horizontal beam slit was installed 1050 mm before the mirror. The slit width was 0.23 mm. Focused beam shape was observed with an imaging plate placed at 1050 mm after the mirror. Beam divergence was 0.09 deg, which results in the unfocused beam width 2.97 mm at the observation point.

Observed beam shapes and their horizontal profiles are shown in Fig. 2. Measurement time was 11160 seconds for each image. The intensities are expressed in “photo-stimulated luminescence (PSL)” per pixel of an imaging plate ( $50 \times 50 \mu\text{m}^2$ ). Focused beam width was 0.25 mm in full width at half maximum, almost reproducing the initial beam size defined by the slit. This result is adequate because the focusing mirror is based on the elliptic arc with eccentric angle around 90 degree. Focused peak intensity was 6 times the unfocused average intensity. Note that the tail of the focused beam is no more than that of the unfocused beam profile, which suggests that the focusing mirror produces little diffuse scattering. Background PSL values randomly dispersed between  $10^{-4}$  and  $10^{-2}$  and were neglected in the analysis.

Figure 3(a) compares a time-of-flight (TOF) spectrum of the focused beam with that of the unfocused one, which were measured with a  $^3\text{He}$  point detector. (Sharp dips are attributed to Bragg reflections by monochromators of upstream instruments in the C-2 beam line.) One

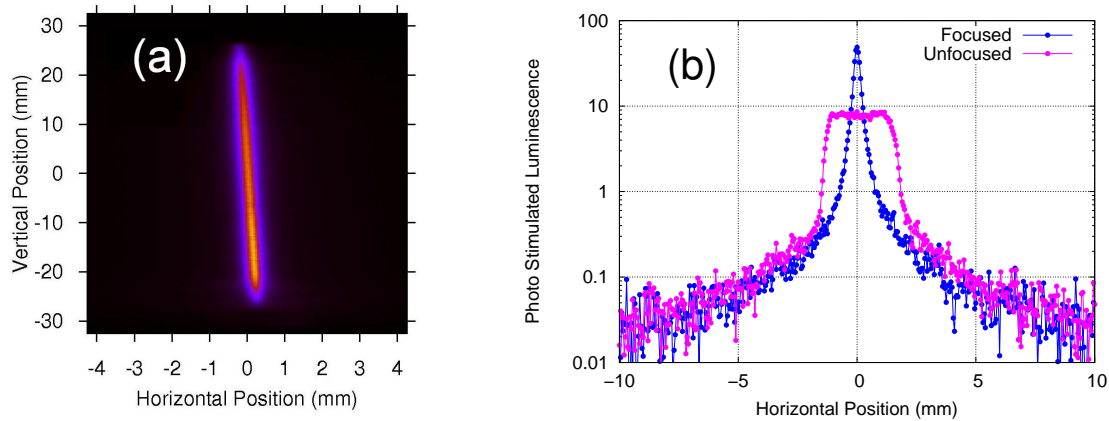


**Figure 2.** (a) 2-dimensional image of the focused beam. Note the scale difference between the two axes. (b) Horizontal intensity profiles of focused and unfocused beam at the vertical center.

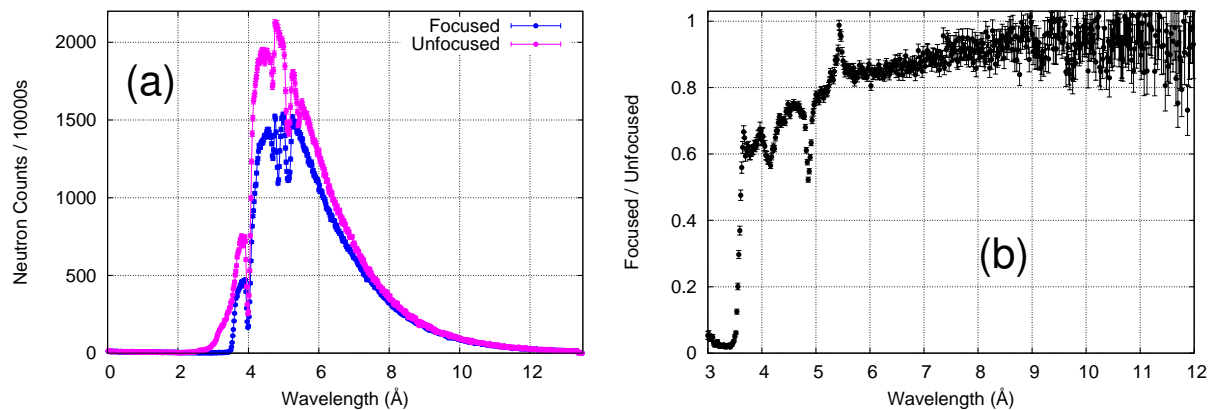


**Figure 3.** (a) TOF spectra of the focused and unfocused beam. (b) Ratio of the two spectra.

can see that neutrons are reflected and focused over a wide wavelength band. The rising of the focused beam profile at wavelength  $\simeq 3.64 \text{ \AA}$  represents the critical wavelength of total reflection by the mirror. Assuming the glancing angle at the mirror is 1.40 degree, the critical wavelength corresponds to critical scattering vector  $Q_z \simeq 0.084 \text{ \AA}^{-1}$  or  $m \simeq 3.87$ . This value is slightly smaller than the specification  $m = 4$ . This difference could be ascribed to an error in the glancing angle because it was adjusted with manual stages and a wide detector-slit (5mm).

Figure 3(b) plots the ratio of the two TOF profiles. (The dips and peaks are attributed to shifts of dip-positions in the TOF spectra which result from changes in the monochromator angles.) We can see a typical reflectivity profile of supermirror. The reflectivity  $\simeq 0.6$  at the critical wavelength also is a typical value. This result suggests that most reflected neutrons are transported to the focal spot without significant loss.

The same measurements were carried out with the slit width  $\simeq 0.43 \text{ mm}$ . Focused beam size was 0.42 mm and peak intensity was 4.6 times the unfocused intensity. Diffuse scattering once again was not significant. TOF and reflectivity measurement yielded similar profiles to the above case.

These results show that our focusing mirror meets the five requirements mentioned above.

#### 4. Future plans and summary

We are developing more efficient focusing mirrors with larger acceptance angles and smaller focal spot sizes. Acceptance angle can be improved by fabricating larger focusing mirrors and/or stacking them. The mirror size, which is now limited by the coating area of our IBS machine, is readily extendable to 400 mm or more in length. Smaller focused beam size can also be obtained by a mirror based on an elliptic arc with smaller eccentric angles. We are also developing two dimensional focusing by figuring elliptic-cylinder surface or combining two elliptic mirrors (Kirkpatrick-Baez mirror).

In summary, we have developed a 1-dimensional elliptic mirror combining the supermirror deposition with ion-beam sputtering and precise elliptic surface figured with the numerically-controlled local wet etching process. Wideband neutrons of  $\lambda > 3.64\text{\AA}$  were focused with focal spot size down to 0.25 mm, peak intensity gain up to 6 and signal-to-noise ratio less than the non-focused beam. Time-of-flight measurements suggest that wideband neutrons are effectively focused to the focal point.

#### Acknowledgments

Authors acknowledge K. Aizawa, S. Takata and I. Tamura for instructions of the CHOP instrument at JRR-3. This work is partially supported by the Industrial Technology Research Grant Program in 2005 from the New Energy and Industrial Technology Development Organization (NEDO) of Japan and a research grant from the Material Tool Engineering Foundation.

#### References

- [1] Ice GE, Hubbard CR, Larson BC, Pang JW, Budai JD, Spooner S and Vogel SC 2005, *Nucl. Instrum. Meth. A* **539** 312-20
- [2] Ice GE, Hubbard CR, Larson BC, Pang JW, Budai JD, Spooner S, Vogel SC, Rogge RD, Fox JH, Donabarger RL, *Mater. Sci. Eng. A* **437** 120-5
- [3] Maruyama R, Yamazaki D, Ebisawa T, Soyama K 2009, *Nucl. Instrum. Meth A* **600** 68-70
- [4] Maruyama R, Yamazaki D, Ebisawa T, Soyama K 2009, *J Appl. Phys.* **105** 083527
- [5] Maruyama R, Yamazaki D, Ebisawa T, Hino M and Soyama K 2007, *Thin Solid Films* **515** 5704-6
- [6] Yamamura K 2007, *Sci. Tech. Adv. Mater.* **8** 158-61
- [7] Yamamura K 2007, *Annals of the CIRP* **56/1** 541-4
- [8] Yamamura K, Nagano M, Takai H, Zettsu N, Yamazaki D, Maruyama R, Soyama K and Shimada S 2009, *Opt. Express.* **17** 6414-20
- [9] Nagano M, Takai H, Yamazaki D, Maruyama R, Soyama K and Yamamura K, in this proceedings.
- [10] Tamura I, Maruyama R, Yamamoto K, Nakamura K, Aizawa K and Soyama K 2008, *JAEA Review* 2008-004 p100